JOURNAL OF CATALYSIS **178,** 658–667 (1998)
ARTICLE NO. CA982200

Surface Redox Characteristics of Mixed Oxide Catalysts Used for Selective Oxidation

Stephen Poulston,* Nicola J. Price,*,[1] Colin Weeks,* Matthew D. Allen,* Peter Parlett,* Menachem Steinberg,† and Michael Bowker*

*Catalysis Research Centre, Department of Chemistry, University of Reading, P.O. Box 224, Whiteknights, Reading, RG6 6AD, United Kingdom; and †Inorganic and Analytical Chemistry, Hebrew University of Jerusalem, Jerusalem 91904, Israel

Received March 5, 1998; revised May 15, 1998; accepted May 15, 1998

A number of mixed-metal oxides have been reduced *in situ* by H_2 and NH_3 at pressures in the range 5×10^{-5} to 1 mbar and temperatures of around 520 K. The oxides studied, $FeSbO_4$, $Bi_2Mo_2O_9$, $VSbO_4$, $Bi_4V_2O_{11}$, and USb_3O_{10}, were chosen as they represent model systems for the catalysts used in the selective oxidation and ammoxidation of alkanes and alkenes. The surface composition was monitored before and after reduction using X-ray photoelectron spectroscopy (XPS). The ease of reducibility of the oxides was $Bi_2Mo_2O_9$ (easiest to reduce), $FeSbO_4$, $VSbO_4$, USb_3O_{10}, and $Bi_4V_2O_{11}$. Following reduction either Bi or Sb metal was observed at the surface of the oxides containing these elements, together with a reduction in the oxidation state of some of the V, Mo, Fe, or U components to 3+, 4+, 2+, and 4+, respectively. Subsequent vacuum annealing between 770 and 820 K resulted in reoxidation of the surface so that the oxidation states of its components were returned to their original value, together with desorption of Bi or Sb. It is believed that diffusion of lattice oxygen to the surface was responsible for this process, with only a relatively thin surface layer of material having been reduced. In some cases the surface composition could not readily be returned to its original value by this annealing process, suggesting limited mobility of the cations at the annealing temperature.

INTRODUCTION

The stability of catalyst materials in both oxidising and reducing atmospheres is of great importance to catalysis. Strong oxidising and reducing gases are involved in many industrial reactions and ammoxidation catalysts in particular operate in the presence of both oxidising (oxygen) and reducing (propene and NH_3) gases. It has been clearly demonstrated that many ammoxidation catalysts produce catalytic oxidation through a redox mechanism involving lattice oxygen with rapid migration of oxide ions from the bulk to the surface maintaining the structure and composition of the active surface phase so enhancing the catalyst lifetime (1). However, prolonged use of these catalysts can eventually result in bulk changes in the structure and composition and loss of catalytic activity/selectivity. Several mechanisms could operate towards catalyst deactivation, including decomposition of active components, formation of different metal oxides, and loss of a particular metal element due to sublimation of a volatile component. All of these mechanisms occur in reducing environments. These processes can be modelled by exposing mixed metal oxides of the type found in commercial ammoxidation catalysts to reducing environments such as H_2 and NH_3. Furthermore, in selective oxidation reactions the diffusion of lattice oxide ions to maintain surface composition can give important indicators to the selectivity of the catalyst (2, 3). The nature of the oxygen species present at the surface of the catalyst is crucial to their catalytic behaviour, and the main aim of this work is to carry out a comparative study of the oxygen stability on a series of mixed metal oxide catalysts. The easier it is to reduce the surface of the catalyst, the more active it is likely to be.

Several studies have investigated the bulk and surface changes of ammoxidation catalysts such as Fe-Sb oxide (4–6), Bi-Mo oxide (7, 8), bismuth-vanadium-molybdenum oxides (2, 3), and iron-containing bismuth molybdovanadates (9) after treatments in a range of chemical environments using X-ray photoelectron spectroscopy (XPS), transmission electron microscopy (TEM), X-ray diffraction (XRD), and temperature-programmed oxidation (TPRO). These studies have helped identify mechanisms for compositional changes in the oxide catalysts and also have given information on the lattice oxygen mobility. The initial stages of this process are particularly suitable for study by surface-sensitive spectroscopies, in particular, XPS. In this study we present XPS data showing changes in the surface composition of a number of model ammoxidation catalysts under reducing conditions of ammonia and hydrogen, and their reoxidation by vacuum annealing.

[1] Corresponding author. E-mail: SCS96NJP@READING.AC.UK.

0021-9517/98 $25.00

EXPERIMENTAL

Catalyst Characterisation

XPS measurements were carried out using a VSW system with a 100-mm radius hemispherical analyser and Al(K_α) photons at a typical base pressure of 5×10^{-9} mbar. The sample was pressed on a stainless steel mesh with a chromel–alumel thermocouple attached, and this was mounted onto a manipulator. The bismuth vanadate spectra were referenced with respect to O(1s) at 529.8 eV. Other spectra were referenced to the adventitious C(1s) line at 284.8 eV. TPD was carried out by radiative heating of the sample from a tungsten filament heater situated close to the rear of the sample at a ramp rate of ~ 3 Ks^{-1}. Desorption profiles were measured using a VG quadrupole mass spectrometer. Gas dosing was carried out with the sample at room temperature by backfilling the chamber. The weight of the catalyst used was typically 0.2 g. In the case of Fe(2p) XPS, the background subtraction method used was a Proctor/Hercules modified Shirley integration (10); otherwise a linear background subtraction was used. Determination of the antimony surface atomic ratio was calculated from the peak area of the Sb(3d) transition after subtraction of the contribution of the overlapping O(1s) peak from the Sb($3d_{5/2}$) peak (assuming a 3 : 2 ratio of $3d_{5/2} : 3d_{3/2}$). It was estimated that the contribution of the O(1s) to this peak was approximately 30%. The V($2p_{3/2}$) peak was used in determination of atomic ratios as the V($2p_{1/2}$) peak is in the energy range of the O(1s) satellite. The relative cross-sectional sensitivities of Sb(3d), Fe(2p), Bi(4f), V(2p), Mo(3d), O(1s), and U(4f) were taken as 4.47, 2.67, 7.63, 1.91, 2.87, 0.71, and 8.48, respectively (11). The XRD powder diffraction data were recorded using an Inel Spectrolab CPS 120 using CuKα radiation and operated at 40 kV and 40 mA.

Catalyst Preparation

Fe-Sb oxide. The SbFe catalyst was prepared by a slurry impregnation method (12). $Fe(NO_3)_3 \cdot 9H_2O$ (35g) was heated to 333 K, at which temperature a solution of iron nitrate in its own water of crystallisation was formed, Sb_2O_3 (11.98 g) was added, the temperature raised to 350 K, and the solution pH was adjusted to 3.0 using aqueous ammonia. The brown solid was recovered by filtration and dried (400 K, 16 h), it was then dried and calcined in air at 1173 K and atmospheric pressure for 7 h to give inter-diffusion of the cations. The XRD data were in good agreement with previous work on $FeSbO_4$ (23).

Bi-Mo oxide. 12.1 g of $Bi(NO_3)_3 \cdot 5H_2O$ and 4.5 ml of concentrated HNO_3 were dissolved in water and the solution made up to 50 cm^3; 4.4 g $(NH_4)_2MoO_4$ was dissolved in 50 cm^3 of water. The molybdenum solution was then added, dropwise with stirring, to the bismuth solution, forming a white precipitate. The pH of 1 was adjusted to 5 (using NH_4OH) and the solution was filtered to give a pale yellow solid that was then washed, dried, and then calcined at 770 K for 2h in air. The compound used had an XRD pattern in agreement with that obtained for the same preparation procedure by others (13), suggesting it was largely $Bi_2Mo_2O_9$, i.e. beta bismuth molybdate with traces of 2 : 3 (alpha) and 2 : 1 (gamma) Bi : Mo.

V-Sb oxide. The catalyst was prepared following the procedure of Nilsson *et al.* (14) by adding a warm solution of ammonium vanadate (11.6 g dissloved in distilled water) to a suspension of Sb_2O_3 (9.36 g) which was then refluxed for 18 h. Water was evaporated from the slurry using a hot plate until a thick paste was formed. The paste was then dried for 16 h at 383 K and subsequently heated in air at 623 K for 5 h. After sieving, the fraction 150–425 mesh was calcined at 883 K for 3 h. The XRD indicated very small amounts of Sb_2O_3 and a rutile phase consistent with the cation-deficient $Sb_{0.92}V_{0.92}O_4$ structure previously reported from XRD measurements by Hansen *et al.* (15). Unlike the reports of Nilsson *et al.* (14) no Sb_2O_4 could be detected in the XRD.

Bi-V oxide. 19.402 g of bismuth nitrate was dissolved in distilled water and slowly added to a solution of 2.34 g of ammonium metavanadate in water. The pH was then adjusted to 11 with ammonia and the solution filtered; the resulting precipitate was washed with water and, then, acetone before drying in an oven at 383 K. The resulting yellow powder was then ground with a pestle and mortar before being calcined for 1 h at 573 K. The oxide was then ground again and calcined for 15 h at 973 K and left to cool in the furnace. The resulting compound was a bright orange powder. XRD analysis of the resulting compound was in good agreement with previous data for $Bi_4V_2O_{11}$ (16, 17).

U-Sb oxide. A solution of uranyl nitrate $[UO_2(NO_3) \cdot 6H_2O]$ (8.8g) was dissolved in 70% nitric acid. Antimony (III) oxide (8.7 g) was added to the nitric acid solution and diluted with triply distilled water and refluxed for 40 h. After cooling, a solution of 25% ammonium hydroxide was added until a pH of 8 was reached. The resulting precipitate was filtered, dried for 20 h at 393 K, heated in air to 700 K for 26 h, cooled to room temperature, and then calcined in air at 1173 K for 23 h. The structure was confirmed using XRD as USb_3O_{10}.

RESULTS AND DISCUSSION

1. Bi-Mo Oxide

XPS spectra of the Bi-Mo oxide sample after vacuum annealing to 820 K are shown in Figs. 1a (Mo) and 2a (Bi). The main Mo($3d_{5/2}$) peak occurred at 232.5 eV characteristic of Mo^{6+}, reported values of MoO_3 being in the range 232.3–232.8 eV BE and 232.5 eV for $Bi_2Mo_2O_9$ (9). Also distinguished was a small but significant peak at 229.5 eV,

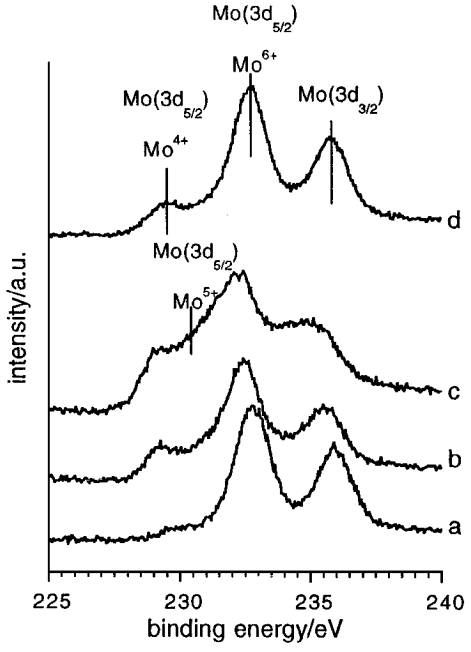

FIG. 1. XPS spectra of the Mo(3d) peak from $Bi_2Mo_2O_9$ after various *in situ* treatments: (a) vacuum annealed to 820 K; (b) heated at 620 K for 10 min in 1×10^{-4} mbar NH_3; (c) heated at 520 K for 10 min in 5×10^{-5} mbar H_2; (d) H_2-reduced sample heated to 823 K for 10 s.

indicating the presence of a small amount (<5%) of Mo^{4+} (MoO_2 has a reported $Mo(3d_{5/2})$ binding energy of 229.1–229.6 eV and there are no reports of a stable oxide phase below MoO_2 (18)). The observation of small amounts of reduced Mo is not surprising, considering the large number of stable phases of molybdenum oxide that exist in the stoichiometry range between MoO_3 and MoO_2 (19). Brazdil *et al.* (20) have suggested that on reduction of $Bi_2Mo_2O_9$ a reaction occurs at the surface as shown in Eq. [1] which produces Mo species with an oxidation state of 4+:

$$Bi_2Mo_2O_9 \rightarrow Bi_2MoO_{6-x} + MoO_{3-y} + (x + y)[O]. \quad [1]$$

The corresponding Bi(4f) peak, Fig. 2a, exhibited only one chemical state with a $Bi(4f_{7/2})$ BE of 158.9 eV characteristic of Bi^{3+}, literature values for Bi^{3+} in Bi_2MoO_9 being 158.0–158.8 eV BE. Quantitative XPS analysis of the fresh sample after annealing in vacuum to 820 K indicated an atomic ratio of $Bi_{1.3}MoO_{3.7}$, the oxygen ratio is slightly low, presumably due to surface reduction. The observed Bi : Mo ratio is in reasonable agreement with the work of Arora *et al.* (21) who suggest that the surface composition is close to that of the bulk for a range of Bi : Mo ratios.

No significant change was observed in the XPS spectra for reduction in 3×10^{-5} mbar NH_3 for 10mins at 470 K. However, with 1×10^{-4} mbar NH_3 at 620 K there was significant change in the Mo(3d) spectra (Fig. 1b) with a large increase in the Mo^{4+} signal relative to Mo^{6+}, the binding energy of the 4+ state also appeared at ~0.5 eV lower binding energy though this shift still leaves the binding energy too high for Mo metal. No significant change was observed in the Bi(4f) signal. Heating the sample in vacuum to 820 K did not result in any significant loss of the Mo^{4+} intensity although there was a shift of ~+0.5 eV in the $Mo(3d_{5/2})$ peak associated with this state back to the original 4+ BE. Prolonged annealing at 820 K significantly reduced the intensity of the 4+ state.

Hydrogen was found to be a far more powerful reducing agent. Heating the sample for 10 min at 5×10^{-5} mbar H_2 at 520 K led to significant reduction of both the Bi and Mo components of the surface. An additional set of Bi(4f) doublets was observed, Fig. 2b, at 156.7/162.0 eV, 2.3 eV lower BE than the peaks associated with Bi^{3+} and these can be assigned to formation of metallic bismuth. Approximately half the Bi(4f) peak intensity occurs as the metallic state in this case. Hydrogen reduction also results in ~1/2 the Mo being converted to a lower oxidation state including both 4+ and 5+ Mo, this represents a far higher level of reduction than for the NH_3 reducing conditions described above. The 5+/4+ region also occurs as a rather broad feature, Fig. 1c, although deconvolution allowed for the determination of the binding energies of the 4+ and 5+ states to be made (229.1 eV and 230.2 eV, respectively). The position of the Mo^{6+} signal remained at 232.3 eV binding energy. Flashing the sample to 823 K led to a significant reduction in the $Mo^{4+/5+}$ peak intensity though again not its complete removal, Fig. 1d. The residual $Mo^{4+/5+}$ peak was comparable in intensity to that left after NH_3 reduction and flashing

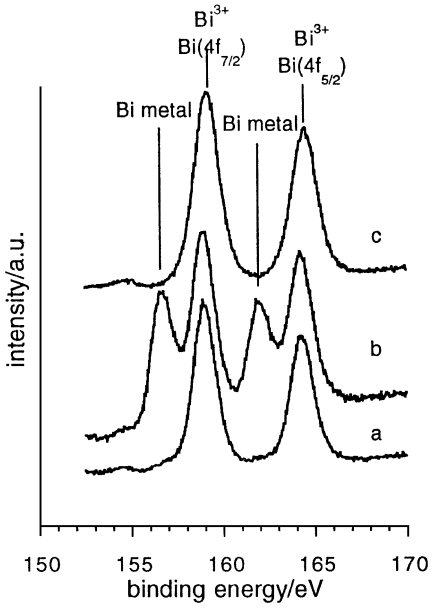

FIG. 2. XPS spectra of the Bi(4f) peak from $Bi_2Mo_2O_9$ after various *in situ* treatments: (a) vacuum annealed to 820 K; (b) heated at 520 K for 10 min in 5×10^{-5} mbar H_2; (c) again vacuum annealed to 820 K.

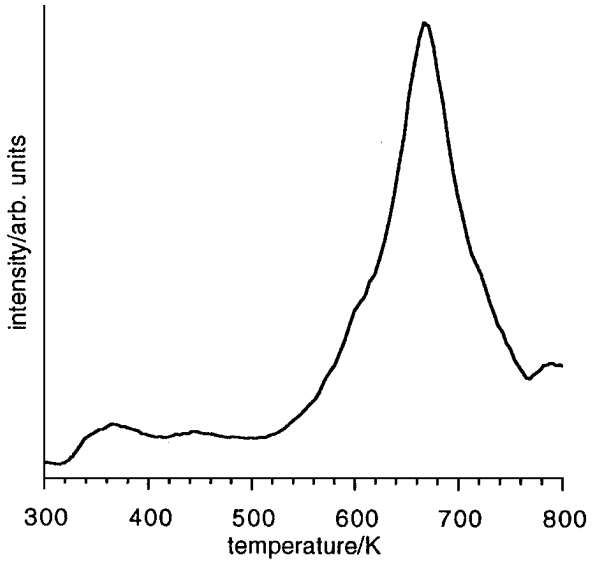

FIG. 3. TPD trace showing mass 104 (Bi^{2+}), indicating Bi desorption following reduction of $Bi_2Mo_2O_9$ for 10 min in 5×10^{-5} mbar H_2 at 520 K.

to the same temperature. This brief heating did, however, completely remove any trace of a metallic Bi state in the Bi(4f) spectra, Fig. 2c. TPD data of the hydrogen reduced sample shown in Fig. 3 reveal an intense Bi desorption peak at 660 K. This demonstrates that the Bi metal generated on reduction is at least partly desorbed on subsequent annealing. Prolonged heating at 820 K left some residual Mo^{4+} signal similar to the flashed sample. Most of the reduced molybdenum is therefore reoxidised on vacuum annealing. This is further illustrated by consideration of the ratios of the various oxidation states present in the hydrogen-reduced spectrum and the flashed sample. In the case of the hydrogen-reduced spectrum the ratio of Mo^{4+} to Mo^{6+} is $\sim 1:4$, whereas for the flashed sample the 4+ contribution is significantly reduced ($Mo^{4+}:Mo^{6+} \sim 1:10$). The reoxidation of cations in oxide materials with vacuum annealing is known from surface science studies of a number of oxide materials, the most well-known example probably being TiO_2. In that case reduction of the Ti^{4+} to $Ti^{3+/2+}$ occurs on Ar^+ ion bombardment following the preferential removal of oxygen during sputtering (22). Subsequent vacuum annealing returns the surface Ti to Ti^{4+}.

Reduction of the bismuth to metal and the Mo^{6+} to Mo^{4+} in bismuth-molybdate samples was previously observed by Grzybowska *et al.* (8) after exposing Bi_2MoO_6 to hydrogen at 743 K, although in this case no subsequent sample treatments were reported.

It is interesting to note that after these repeated reduction and annealing procedures the final XPS spectrum was indistinguishable from the initial state, a process which involves not only oxygen diffusion to the surface to produce molybdenum re-oxidation but also cation mobility to restore the surface to the original composition following Bi metal desorption. This indicates that the reduction process only substantially affects a relatively thin layer at the surface perhaps only a few tens of Angstroms in depth which would be sufficient to dramatically alter the catalytic properties of the oxide. The regeneration of the surface composition by vacuum annealing following reduction provides clear experimental evidence for the enhancement of catalyst life by the ability of the catalyst to regenerate the original surface. Brazdil *et al.* (20) have shown that lattice oxygen is highly mobile in bismuth molybdate systems allowing the reoxidation of bulk defects at 700 K. The high mobility of lattice oxygen in molybdate systems may be due to the formation of shear structures which are known to occur in molybdenum oxides (19).

2. Fe-Sb Oxide

We have previously shown (5) that $FeSbO_4$ can be reduced by heating in 2×10^{-4} mbar NH_3 at 520 K for 10 min to produce metallic Sb which can subsequently be desorbed by heating to 773 K leaving the surface enriched in Fe. This procedure produces no significant change in the peak shape of the Fe(2p) signal. Reduction of $FeSbO_4$ by H_2, 2×10^{-4} mbar at 520 K for 10 min, produced metallic Sb which was distinguishable by the appearance of a Sb(3d) doublet shifted by 2.5 eV to lower binding energy than the Sb oxide Sb(3d) peaks, Fig. 4. However, in this case there was also a reduction in the Fe component of the sample. Figure 5 shows the Fe(2p) peaks both before and after hydrogen reduction clearly showing a lower binding energy shoulder after reduction. The shoulder is shifted by $\sim$3 eV

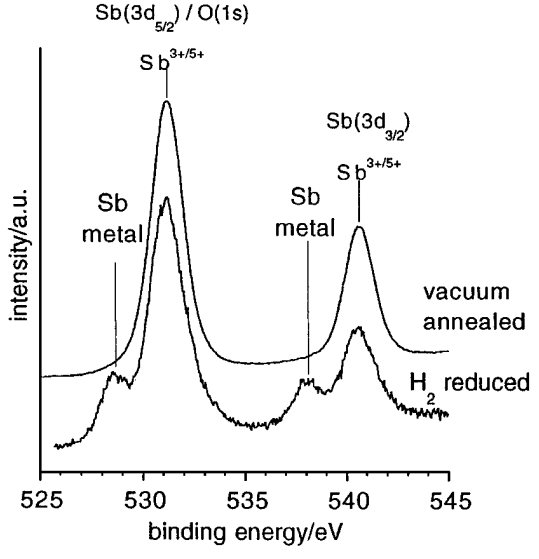

FIG. 4. XPS spectra showing the Sb(3d) peaks of $FeSbO_4$, following vacuum annealing at 770 K and after H_2 reduction (2×10^{-4} mbar H_2 at 520 K for 10 min). The principle $Sb(3d_{5/2})$ peak at 531.5 eV is due to $Sb^{3+/5+}$ and O(1s) and following reduction there is an additional peak due to Sb metal as marked.

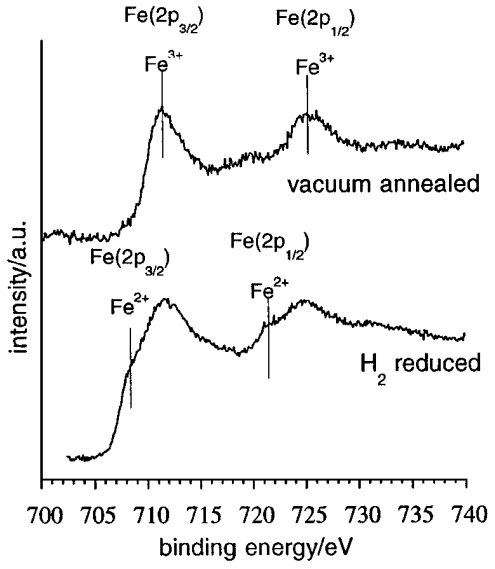

FIG. 5. XPS spectra showing the Fe(2p) peaks of $FeSbO_4$ following vacuum annealing at 770 K and after H_2 reduction (2×10^{-4} mbar H_2 at 520 K for 10 min).

to lower binding energy, i.e. at 709.3 and 722.0 eV BE for the $2p_{3/2}$ and $2p_{1/2}$ peaks, respectively. This indicates the formation of significant amounts of Fe^{2+} at the surface though substantial amounts of Fe^{3+} ($2p_{3/2}$ at 711.5 eV) were still present. Annealing to 770 K removed both the Fe^{2+} shoulder and the Sb metal peaks. Loss of Sb metal can again be attributed to Sb desorption though loss of the Fe^{2+} probably arises from reoxidation to Fe^{3+} by oxygen diffusion from the bulk. Sb desorption was observed in TPD from samples with Sb metal at the surface following reduction (5,6). The H_2 reduction/thermal Sb loss procedure could be repeated to gradually deplete the antimony component of the surface. After each cycle the iron enrichment at the surface increased leading, after several cycles, to an Sb : Fe ratio of 1 : 5.8 compared with 2.6 : 1 for the original surface. XPS spectra for the surface before and after these reduction–desorption cycles are shown in Fig. 6 normalised to the same Sb(3p) peak intensity. As can be seen there is a substantial increase in the Fe(2p) intensity relative to Sb($3p_{3/2}$). Therefore, in contrast to the case of $Bi_2Mo_2O_9$ the cation mobility at the annealing temperature, 770 K, was not sufficient to return the surface composition to its original state. This result is perhaps not surprising considering the calcination temperatures used in preparing the two samples, a procedure which is carried out, in part, to produce intermixing of the cations. For $Bi_2Mo_2O_9$ the calcination temperature was 770 K but for $FeSbO_4$ the temperature required was 1173 K indicating a much lower cation mobility in the latter case. A good indication of cation mobility in the $FeSbO_4$ system can be obtained from XRD experiments by Carbucicchio *et al.* (23) who followed the development of the XRD pattern with increasing calcination temperature of the slurry used in the synthesis of $FeSbO_4$. Calcination at 873 K did not give a pattern and calcination to >1073 K was required in order to obtain lines characteristic of $FeSbO_4$. These results are consistent with the limited cation mobility we have observed at 770 K.

3. V-Sb Oxide

As mentioned above XRD of this material was consistent with the formation of $Sb_{0.92}V_{0.92}O_4$. It is thought that this cation deficient $VSbO_4$ phase contains predominantly Sb^{5+} and $V^{4+/3+}$ (15, 24). However, previous studies (14, 25, 26) have indicated that even in the presence of excess Sb, i.e. Sb-V atomic ratio >1, these catalysts have a surface with a preponderance of V^{5+} and V^{4+} states and a significant amount of Sb^{3+}. Figure 7a shows the Sb(3d) and V(2p) XPS region after vacuum annealing of the freshly prepared sample. The $Sb(3d)_{3/2}$ peak maxima remained constant with heating at 539.8 eV BE, although the V($2p_{3/2}$) peak shifted slightly from 516.4 to 516.0 eV BE on annealing to 773 K. Assignment of these peaks to specific oxidation states of vanadium and antimony is difficult as the Sb 3+ and 5+ oxidation states are within ~0.8 eV of each other and there are a range of possible vanadium phases. Furthermore, an added complication is the difficulty in obtaining a consistent and reliable calibration especially when comparing results from different publications. In an XPS study of a range of vanadium oxide compounds Mendialdua *et al.* (27) suggest that vacuum annealing of polycrystalline V_2O_5 at 823 K results in a surface region of stoichiometry V_6O_{13} and a V($2p_{3/2}$) BE of 516.2, very close to the value of the vacuum annealed sample in Fig. 7a. Mendialdua *et al.* (27) report that a fully oxidised V_2O_5 surface has a V($2p_{3/2}$) BE of 517.0 and a V_2O_3 surface has a V($2p_{3/2}$) BE of 515.15, clearly either side of the BE of the vacuum annealed sample. Sawatzky and Post (28) and Andersson *et al.* (29) have also

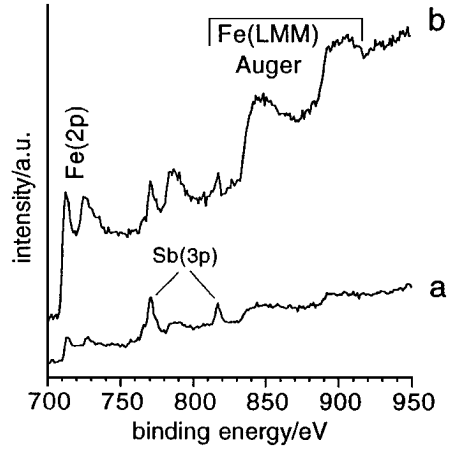

FIG. 6. XPS spectra of $FeSbO_4$: (a) before and (b) after 3 cycles of H_2 (2×10^{-4} mbar H_2 at 520 K for 10 min) reduction and annealing to 770 K. The two spectra are normalised to the same Sb(3p) peak intensity.

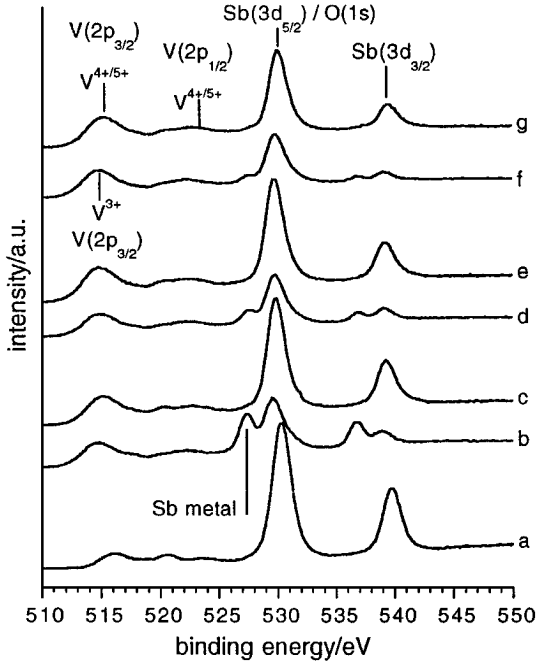

FIG. 7. XPS spectra of $VSbO_4$ showing the Sb(3d) and V(2p) region: (a) after vacuum annealing to 773 K; (b) after heating in 5×10^{-2} mbar H_2 at 520 K for 10 min; (c) H_2-reduced surface after annealing to 823 K; (d) following a second H_2 reduction and (e) re-annealing; (f) following a third H_2 reduction and (g) re-annealing.

carried out XPS measurements on a number of vanadium oxide compounds. Comparison of their results clearly indicates the difficulty in obtaining accurate binding energies for vanadium oxides. For example, in the work of Sawatzky and Post, a BE of 515.7 eV is quoted for V_2O_3, whereas the same value is quoted for the BE of VO_2 in the work of Andersson *et al*. The data presented here are consistent with the presence of both V^{4+} and V^{5+} species at the surface giving an average oxidation state which is probably close to that of the surface V_6O_{13} phase suggested by Mendialdua *et al*. (27) for vacuum annealed V_2O_5. The small reduction in the $V(2p_{3/2})$ BE on vacuum annealing would be consistent with a reduction of the surface from only V^{5+} to a mixture of V^{4+} and V^{5+} on annealing to 823 K. The Sb XPS spectrum is consistent with the presence of both 3+ and 5+ for reasons which are described in the H_2 reduction data below.

Hydrogen reduction, which led to a significant change in the XPS spectra, was considerably more difficult for the V-Sb oxide catalyst than for either Sb-Fe or Bi-Mo. Significant changes were not observed until the catalyst was heated at 523 K in 5×10^{-2} mbar H_2 for 10 min. This procedure resulted in a reduction of the surface to produce Sb metal, indicated by the appearance of an $Sb(3d_{5/2})$ peak at 527.4 eV BE and a lowering of the $V(2p_{3/2})$ BE from 516.2 to 514.7, indicating the presence of V^{3+} at the surface, Fig. 7b. It is also noteworthy that the $Sb(3d_{3/2})$ peak of the oxidised component of the Sb shifts to lower BE on H_2 reduction, a process which can be explained by an increase in the Sb^{3+} to Sb^{5+} ratio in the surface region. If the reduced surface is heated in vacuum to 823 K, Fig. 7c, the Sb metal is desorbed and was not observed in the subsequent XPS spectrum. There is also an increase in the $V(2p_{3/2})$ BE, although not quite up to its original value, indicating a partial re-oxidation of the vanadium at the surface. Repetitions of the H_2 reduction anneal cycles are also shown in Figs. 7d–g and they show that the reduction of the Sb to metal becomes progressively more difficult as less and less Sb metal is produced at the surface. Also apparent is an increase in the V : Sb ratio with this reduction/anneal cycling. Quantitative XPS indicates a decrease in the Sb : V ratio from 2.6 : 1 in the vacuum-annealed sample to 1.5 : 1 following the final reduction/anneal cycle. The loss of Sb from the near surface region is not compensated for by diffusion of Sb from the bulk at this annealing temperature. This is in contrast to the Bi-Mo case where loss of the volatile Bi component in the near surface region is reversed on vacuum annealing by Bi diffusion from the bulk to re-establish the original Bi-Mo ratio at the surface. From the reduction experiments on the iron antimonate and bismuth molybdate samples it is clear that lower pressures are needed for reduction in H_2 than reduction in NH_3. In our experimental apparatus a NH_3 pressure higher than 1×10^{-2} mbar was not possible so NH_3 reduction experiments were not performed for vanadium antimonate.

4. Bi-V Oxide

XPS spectra of the Bi-V sample following vacuum annealing to 773 K are shown in Figs. 8 (Bi) and 9 (V). The

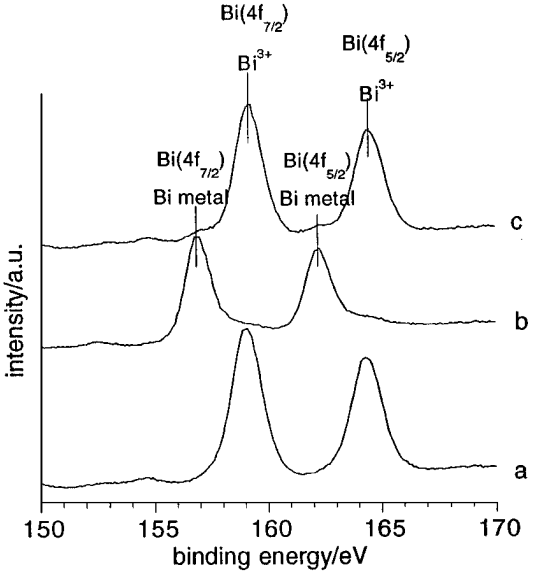

FIG. 8. XPS spectra of $Bi_4V_2O_{11}$ showing the Bi(4f) region: (a) after vacuum annealing to 773 K; (b) after heating in 1 mbar H_2 at 523 K for 10 min; (c) H_2-reduced surface after annealing to 773 K.

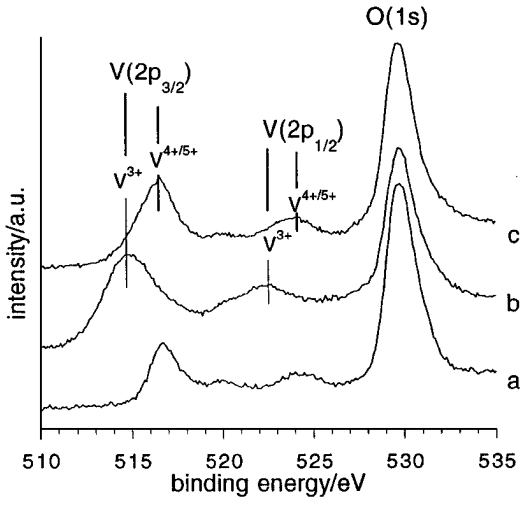

FIG. 9. XPS spectra of $Bi_4V_2O_{11}$ showing the V(2p) region: (a) after vacuum annealing to 773 K; (b) after heating in 1 mbar H_2 at 523 K for 10 min; (c) H_2-reduced surface after annealing to 773 K.

binding energy of the $V(2p_{3/2})$ peak at 516.5 eV again indicates an mix of 5+ and 4+ vanadium oxidation states, as in the case of the vanadium antimonate sample. XPS data of $Bi_4V_2O_{11}$ by Aghabozorg *et al.* also indicated vanadium 4+ and 5+ at the surface (30). The $Bi(4f_{7/2})$ BE of 159.0 eV indicates Bi^{3+} at the surface. Quantitative analysis of the XPS data gives an atomic ratio of Bi : V of 2.3 : 1 in the surface region representing no significant segregation effect, compared with the bulk composition of $Bi_4V_2O_{11}$. The XPS results of Arora *et al.* (21) suggest a bismuth enrichment at the surface of their bismuth-vanadate samples, although the catalyst composition employed in this work was not used by Arora *et al.*

The bismuth vanadate sample was far more difficult to reduce than $VSbO_4$, $FeSbO_4$, or $Bi_2Mo_2O_9$ with conditions of 1 mbar H_2 at 523 K being required before significant changes in the XPS spectra were observed. As shown in Fig. 8 b this procedure resulted in the observation of only Bi metal in the XPS spectra ($Bi(4f_{7/2})$ at 156.9 eV) with no discernible signal from Bi^{3+}. There was, therefore, an almost complete depletion of Bi oxide within ~30 Å of the surface. In addition, the $V(2p_{3/2})$ peak was shifted to 514.9 eV, indicating the formation of V^{3+}, Fig. 9b. Subsequent vacuum annealing to 773 K resulted in the reappearance of only Bi^{3+} in the Bi(4f) XPS spectra, Fig. 8c, and a shift in the $V(2p_{3/2})$ back to 516.5 eV, Fig. 9c, indicating a substantial reoxidation of the surface. However, following this annealing the surface composition was altered, with an increase in the V : Bi ratio relative to the original value before reduction (from 1 : 2.3 to 2 : 1). Repeated cycles of H_2 reduction again led to surface reduction, similar to the case shown in Fig. 8 and, after annealing to 773 K, an increase in the V : Bi ratio.

It is interesting to compare these results with the temperature-programmed reduction and oxidation data of Moro-oka on $BiVO_4$ (31). Using XRD analysis to distinguish changes in the catalyst composition following hydrogen reduction and re-oxidation they showed metallic Bi produced after hydrogen reduction, although this phase was removed by subsequent re-oxidation at 723 K. Repeated cycles of this procedure resulted in the formation of a new, although unidentified phase in the XRD pattern as a result of a decomposition of the catalyst structure. This process was, however, impeded in molybdenum-doped compounds. These results demonstrate, in agreement with our XPS data, that the surface of the $Bi_4V_2O_{11}$ sample was not able to return to its original composition following reduction and subsequent annealing.

5. U-Sb Oxide

XPS spectra of the Sb(3d) and U(4f) regions of a USb_3O_{10} catalyst sample are shown in Figs. 10 and 11, respectively. Initially spectra were recorded of the fresh sample which had been vacuum annealed to ~773 K. The binding energy of the $Sb(3d_{5/2})$ peak in the vacuum annealed sample

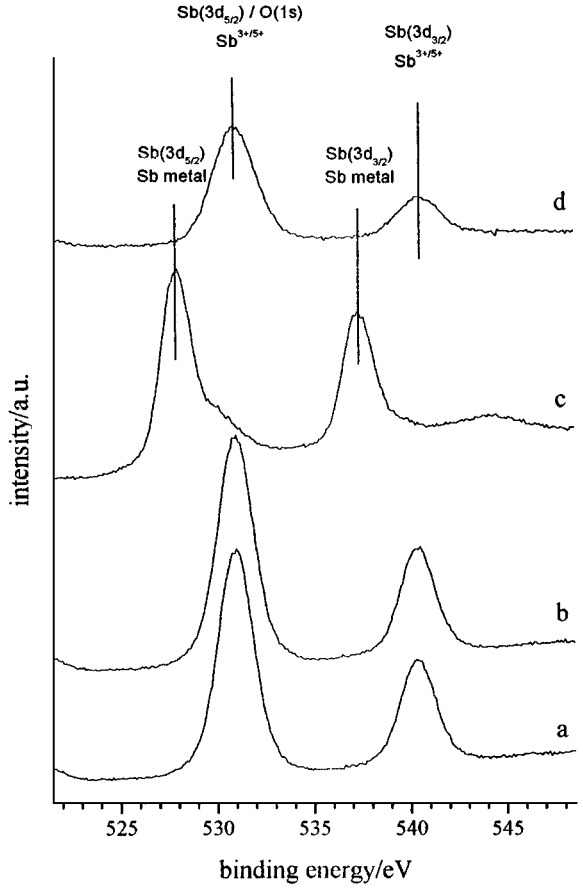

FIG. 10. XPS spectra of USb_3O_{10} showing the Sb(3d) region: (a) after vacuum annealing to 773 K; (b) after heating in 10^{-2} mbar H_2 at 523 K for 10 min; (c) after heating in 0.5 mbar H_2 at 523 K for 10 min; (d) H_2-reduced surface after annealing to 723 K.

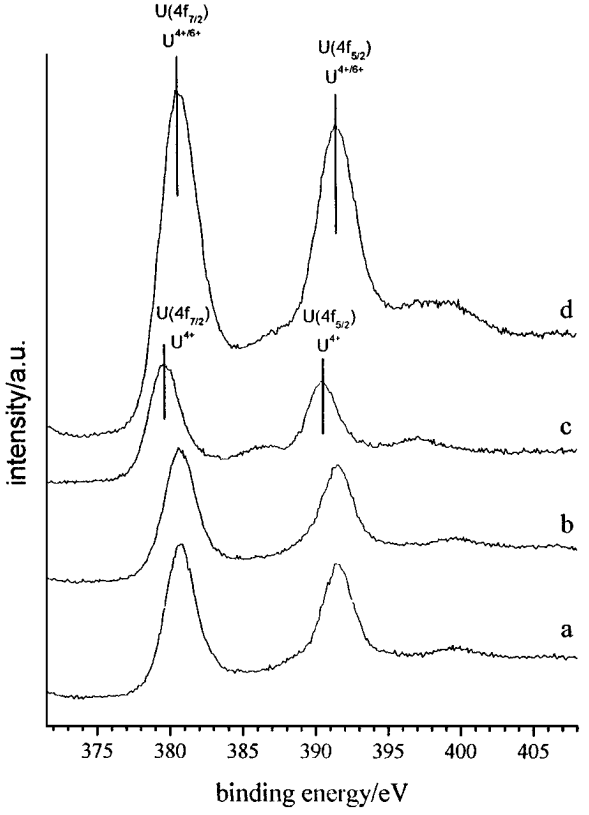

FIG. 11. XPS spectra of USb_3O_{10} showing the U(4f) region: (a) after vacuum annealing to 773 K; (b) after heating in 10^{-2} mbar H_2 at 523 K for 10 min; (c) after heating in 0.5 mbar H_2 at 523 K for 10 min; (d) H_2-reduced surface after annealing to 723 K.

(Fig. 10a) at ~530.9 eV is characteristic of antimony present with an oxidation state of either 3^+ or 5^+. The U($4f_{7/2}$) binding energy at 380.7 eV suggests that uranium is not present exclusively in its highest oxidation state (6^+), but exists as a mixed-valence oxide containing both U^{4+} and U^{6+}. Literature values for the U(4f) binding energy in uranium oxides (11) are reported as being somewhere between 380.0 eV (UO_2) and 381.7 eV (UO_3). Several mixed valence oxides of uranium are known which contain both U^{4+} and U^{6+} (e.g., pitch blende U_3O_8, with a uranium BE of 381.0 eV). Treatment of the catalyst with 10^{-2} mbar of hydrogen at 523 K for 10 min resulted in no observable changes in the antimony or uranium XPS spectra (Figs. 10b and 11b). However, a significant change in both the U(4f) and Sb(3d) spectra was observed upon treatment of the catalyst with pressures of 0.5 mbar of hydrogen and annealing to 523 K for 10 min. Figures 10c and 11c show the Sb(3d) and U(4f) spectra following the aforementioned treatment. Clearly both the metal oxides are reduced, each by significantly differing degrees. In the case of the antimony oxide a shift of ~3 eV to a lower binding energy indicates reduction of the antimony oxide to metallic antimony, although a little of the antimony oxide remains, indicated by a slight, higher binding energy shoulder to the main peak. A less dramatic downward shift in binding energy of ~1 eV to 379.6 eV is evident for the uranium oxide, although the degree of reduction is significant with no discernible shoulder present on the high binding energy side of the U(4f) photoelectron peaks; i.e., all the initial uranium oxide has been reduced, probably to mostly U^{4+}. The binding energy observed is clearly too high to suggest the presence of metallic uranium (binding energy of 377.2 eV).

Vacuum annealing of the catalyst to a temperature of 773 K results in the regeneration of the original antimony and uranium oxides, although the relative amounts of each at the surface are clearly different (Figs. 10d and 11d). During annealing, antimony metal is desorbed from the surface of the catalyst, resulting in an enrichment of uranium (oxide) at the surface. Indeed, quantitative analysis of the XPS spectra (peak areas) confirm that the Sb/U ratio in the catalyst is reduced, falling from an Sb : U ratio of 4.6 : 1 in the initial catalyst to 1 : 1.9 in the reduced/vacuum annealed catalyst.

6. Comparison with Temperature Programmed Reduction (TPR)

It is interesting to compare the above XPS results with TPR experiments which are commonly used to investigate the oxygen availability of oxide catalysts and show the bulk reducibility of the oxides studied. Figure 12 shows the TPR profiles for the oxides used in this study. Bulk reduction of

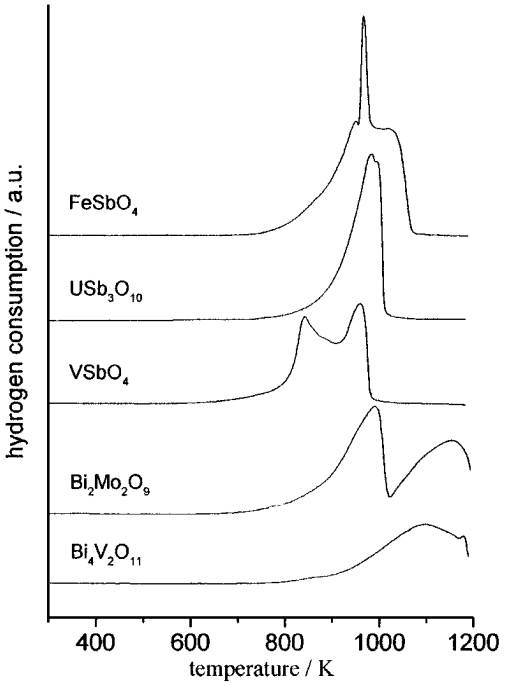

FIG. 12. Temperature-programmed reduction traces for $Bi_4V_2O_{11}$, $VSbO_4$, USb_3O_{10}, $FeSbO_4$, and $Bi_2Mo_2O_9$. Ramp rate of 10 K · min^{-1}; flow rate 10 ml · min^{-1} of 5% H_2/95% He.

the oxides begins at ~750 K, considerably above the temperature of 520 K required to observe hydrogen reduction in the XPS results outlined above. At 520 K there is no indication of significant hydrogen consumption. It is clear, therefore, that the XPS results are monitoring the initial stages of surface reduction in these materials. The $VSbO_4$ seems to be the easiest sample to reduce according to the TPR results, although from the XPS data the surface of the $FeSbO_4$ and Bi_2MoO_9 samples were considerably easier to reduce than $VSbO_4$. The ease of surface reducibility is therefore not readily determined from the bulk reduction represented in our TPR profiles.

CONCLUSIONS

Using XPS we have demonstrated the relative ease with which several mixed metal oxides can be reduced following *in situ* treatments involving heating in H_2 at temperatures below 550 K and pressures up to 1 mbar of H_2. These results are summarised in Table 1. The $Bi_2Mo_2O_9$ was the easiest to reduce, followed by $FeSbO_4$, $VSbO_4$, then USb_3O_{10} and $Bi_4V_2O_{11}$. This correlates with the fact that Bi-Mo and Fe-Sb type catalysts are used for the commercial (amm)oxidation reactions, while the other catalysts are not so active. Reduction under these conditions resulted in the formation of Bi and Sb metals at the surface which could be desorbed by vacuum annealing and so provide a mechanism for changes in the oxide composition. The ease with which the surface could be returned to its original composition by vacuum annealing varied significantly, with $Bi_2Mo_2O_9$ achieving this readily while the other oxides could not be returned to their original composition by vacuum annealing at 773 K. This shows that reduction and desorption of Sb/Bi can produce a surface region which is depleated in Sb/Bi. This process is represented schematically in Fig. 13.

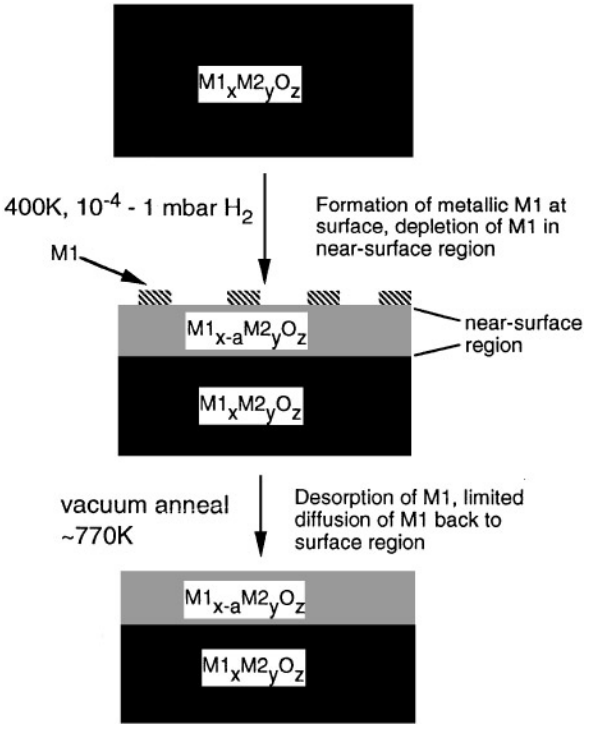

FIG. 13. Schematic representation of the changes in surface composition caused by H_2 reduction and subsequent vacuum annealing of the mixed oxide catalysts of general formula $M1_xM2_yO_z$, where M1 is either Sb or Bi and M2 is V, U, or Mo. The figure shows formation of a near surface region (i.e., XPS analysis region) enriched in the nonvolatile metal which was the case for all the oxides except $Bi_2Mo_2O_9$.

Comparison with temperature-programmed reduction experiments indicates that our XPS observations record the initial stages of reduction involving a relatively thin surface layer. From these results it is clear that substantial changes in the surface composition of these oxides can be produced

TABLE 1

Oxidation States of Metal Atoms at the Surface of Four Mixed Oxides Following Vacuum Annealing and *in situ* Reduction in H_2

Sample	Reduction treatment	Oxidation state of surface species		Surface stoichiometry vacuum annealed
		Vacuum annealed	After H_2 reduction	
Bismuth molybdate	5×10^{-5} mbar H_2, 520 K	Bi3+, Mo6+, 4+	Bi metal, Bi3+, Mo6+, 5+, 4+	Bi : Mo 1.3 : 1
Iron antimonate	2×10^{-4} mbar H_2, 520 K	Fe3+, Sb5+, 3+	Fe3+, 2+, Sb5+, 3+, and Sb metal	Sb : Fe 2.6 : 1
Vanadium antimonate	5×10^{-2} mbar H_2, 520 K	V5+, 4+, Sb5+, 3+	V5+, 4+, 3+, Sb5+, 3+, and Sb metal	Sb : V 2.6 : 1
Uranium antimonate	0.5 mbar H_2, 520 K	U4+, 6+, Sb5+, 3+	U4+, Sb5+, 3+ and Sb metal	Sb : U 4.6 : 1
Bismuth vanadate	1 mbar H_2, 520 K	Bi3+, V5+, 4+	Bi metal, V5+, 4+, 3+	Bi : V 2.3 : 1

Note. The oxides are ranked in the order of their ease of reducibility, i.e., most reducible at the top of the table.

under conditions which are significantly less severe both in pressure and temperature than can be monitored using XRD or TPR.

ACKNOWLEDGMENTS

The authors acknowledge financial support from the University of Reading, the EPSRC, and BASF plc.

REFERENCES

1. Moro-oka, Y., Ueda, W., He, D-H., *in* "Dynamic Processes on Solid Surfaces" (K. Tamaru, Ed.), p. 283. Plenum, New York, 1993.
2. Guerrero-Ruiz, A., Rodriguez-Ramos, I., Ferreira-Aparicio, P., and Volta, J. C., *Catal. Lett.* **45**, 113 (1997).
3. Ueda, W., Asakawa, K., Chen, C-L., Moro-oka, Y., and Ikawa, T., *J. Catal.* **101**, 360 (1986).
4. Bithell, E. G., Doole, R. C., Goringe, M. J., Allen, M. D., and Bowker, M., *Phys. Stat. Sol. (a)* **146**, 461 (1994).
5. Allen, M. D., Poulston, S., Bithell, E. G., Goringe, M. J., and Bowker, M., *J. Catal.* **163**, 204 (1996).
6. Allen, M. D., and Bowker, M., *Catal. Lett.* **33**, 269 (1995).
7. Zhang, L., Liu, D., Yang, B., and Zhao, J., *Appl. Catal. A* **117**, 163 (1994).
8. Grzybowska, B., Haber, J., Marczewski, W., and Ungier, L., *J. Catal.* **42**, 327 (1976).
9. Gazzoli, D., Anichini, A., De Rossi, S., Inversi, M., Lo Jacono, M., Porta, P., and Valigi, M., *J. Catal.* **119**, 277 (1989).
10. Proctor, A., and Hercules, D. M., *Appl. Spectrosc.* **38**, 505 (1984).
11. Moulder, J. F., Stickle, W. F., Sobol, P. E., and Bomben, K. D., "Handbook of X-ray Photoelectron Spectroscopy," Perkin-Elmer, Eden Prairie, MN, 1992.
12. Aso, I., Furukawa, S., Yamazoe, N., and Seiyama, T., *J. Catal.* **64**, 29 (1980).
13. Batist, Ph. A., Bouwens, J. F. H., and Schuit, G. C. A., *J. Catal.* **25**, 1 (1972).
14. Nilsson, R., Lindblad, T., and Andersson, A., *J. Catal.* **148**, 501 (1994).
15. Hansen, S., Ståhl, K., Nilsson, R., and Andersson, A., *J. Solid State Chem.* **102**, 340 (1993).
16. Joubert, O., Jouanneaux, A., and Ganne, M., *Mater. Res. Bull.* **29**, 174 (1994).
17. Bhattacharya, A. K., Mallick, K. K., and Thomas, P. A., *Solid State Commun.* **91**, 357 (1994).
18. Greenwood, N. N., and Earnshaw, A., "Chemistry of the Elements," p. 1175. Pergamon, Elmsford, NY, 1984.
19. Vincent, H., and Marezio, M., *in* "Low-Dimensional Electronic Properties of Molybdenum Bronzes and Oxides" (C. Schlenker, Ed.), p. 49. Kluwer, Dordrecht, 1989.
20. Brazdil, J. F., Suresh, D. D., and Grasselli, R. K., *J. Catal.* **66**, 347 (1980).
21. Arora, N., Deo, G., Wachs, I. E., and Hirt, A. H., *J. Catal.* **159**, 1 (1996).
22. Idriss, H., and Barteau, M. A., *Catal. Lett.* **26**, 123 (1994).
23. Carbucicchio, M., Centi, G., and Trifiro, F., *J. Catal.* **91**, 85 (1985).
24. Birchall, T., and Sleight, A. W., *Inorg. Chem.* **15**, 868 (1976).
25. Andersson, A., Andersson, S. L. T., Centi, G., Grasselli, R. K., Santi, M., and Trifiro, F., *Appl. Catal. A* **113**, 43 (1994).
26. Centi, G., and Perathoner, S., *Appl. Catal. A* **124**, 317 (1995).
27. Mendialdua, J., Casanova, R., and Barbaux, Y., *J. Electron Spectrosc. Relat. Phenom.* **71**, 249 (1995).
28. Andersson, S. L. T., *J. Chem. Soc. Faraday Trans.* **75**, 1356 (1979).
29. Sawatzky, G. A., and Post, D., *Phys. Rev. B.* **20**, 1546 (1979).
30. Aghabozorg, H. R., Flavell, W. R., and Sakakini, B. H., *J. Catal.* **167**, 164 (1997).
31. Moro-oka, Y., *in* "New Aspects of Spillover Effect in Catalysis," (T. Inui, K. Fujimoto, T. Uchijima, M. Masai, Eds.), p. 95. Elsevier, Amsterdam, 1993.